# The Structure of the Cytidine Deaminase−Product Complex Provides Evidence for Efficient Proton Transfer and Ground-State Destabilization[†,‡]

Shibin Xiang,[§] Steven A. Short,[||] Richard Wolfenden,[§] and Charles W. Carter, Jr.*[,§]

*Department of Biochemistry and Biophysics, University of North Carolina at Chapel Hill, Chapel Hill, North Carolina 27599-7260, and Molecular Sciences, Venture 31, Glaxo-Wellcome, 5 Moore Drive, Research Triangle Park, North Carolina 27709*

*Received December 17, 1996; Revised Manuscript Received January 29, 1997*[⊗]

ABSTRACT: Crystal structures of the cytidine deaminase−uridine product complex prepared either by cocrystallizing enzyme with uridine or by diffusing cytidine into ligand-free crystals show that the product binds as a 4-ketopyrimidine. They reveal four additional features of the catalytic process. (1) A water molecule bound to a site previously observed to bind the incoming 4-$NH_2$ group represents the site for the leaving ammonia molecule. The conserved Pro 128 accommodates both moieties by orienting the carbonyl group of the previous residue. (2) The Glu 104 carboxylate group rotates from its hydrogen bond to the O4 hydroxyl group in transition-state analog complexes, forming a new hydrogen bond to the leaving group moiety. Thus, after stabilizing the hydroxyl group in the transition state, Glu 104 transfers a proton from that group to the leaving amino group, promoting enol-to-keto isomerization of the product. (3) Difference Fourier comparisons with transition-state complexes indicate that the pyrimidine ring rotates toward the zinc by ∼10°. The active site thus "pulls" the ring and 4-$NH_2$ group in opposite directions during catalysis. To preserve coplanarity of the 4-keto group with the pyrimidine ring, the N1−C1′ glycosidic bond bends by ∼19° out of the ring plane. This distortion may "spring-load" the product complex and promote dissociation. Failure to recognize a similar distortion could explain an earlier crystallographic interpretation of the adenosine deaminase−inosine complex [Wilson, D. K., & Quiocho, F. A. (1994) *Nat. Struct. Biol. 1*, 691−694]. (4) The Zn−$S_\gamma$132 bond, which lengthens in transition-state complexes, shortens as the O4 atom returns to a state of lower negative charge in the planar product, consistent with our previous proposal that this bond buffers the zinc bond valence, compensating buildup of negative charge on the oxygen nucleophile during catalysis.

We report here the structural characterization of the product complex for *Escherichia coli* cytidine deaminase (CDA).[1] CDA catalyzes hydrolytic deamination of cytidine to uridine by increasing the rate roughly $10^{11}$-fold (Frick et al., 1987). Considerable effort has been devoted to studies of the catalytic mechanism of nucleoside deaminases (CDA) and adenosine deaminase (ADA) (Cohen & Wolfenden, 1971a,b; Marquez et al., 1980; Liu et al., 1981; Ashley & Bartlett, 1984; Kim et al., 1986; Wilson et al., 1991; Wilson & Quiocho, 1993; Betts et al., 1994; Carlow et al., 1995; Xiang et al., 1995, 1996; Carlow et al., 1996). The work reported here was done in the context of a comprehensive study of structural differences between the interaction of CDA with ligands resembling different stages of catalysis. We have studied stable crystal structures representing intermediate catalytic states achieved by sectioning the catalytic process with different inhibitors. These structures include the ground state, represented by CDA complexed to the substrate analog 3-deazacytidine (DAC; Xiang et al., 1996), and the transition state, represented by CDA complexed to the transition-state analogs, zebularine (ZEB-OH; Xiang et al., 1995) and 5-fluorozebularine (FZEB-OH; Betts et al., 1994). In the ground-state complex CDA·DAC, a binding site for the incoming amino group was identified, and a water molecule was found trapped in the active site and aligned properly for addition to C4. In the transition-state-like complexes CDA·ZEB-OH and CDA·FZEB-OH, this water molecule attacks C4 to form a covalent tetrahedral adduct with many features of the putative transition state.

Here, we analyze the structure of the complex formed between cytidine deaminase and a compound actually encountered during deamination: the product, rather than an inhibitor. It is commonly assumed to be difficult to "trap" complexes that actually occur on an enzyme-catalyzed reaction path. The possibility of characterizing an enzyme−ligand complex related to catalysis depends on the stability of that complex. This, in turn, depends both on the stability of the ligand itself, relative to other species with which it might interconvert, and on the affinity with which these are held by the enzyme. In the case of the nucleoside deaminases, these two free energies are known. The $K_i$ for product inhibition of CDA by uridine is $8 \times 10^{-4}$ M (Carlow et al., 1996). Moreover, conversion of cytidine to uridine in solution is favored by a free energy change of −5.8 kcal/mol (Cohen & Wolfenden, 1971b). Together, these findings

[†] This work was supported by a grant from the American Cancer Society (BE-54B).

[‡] Coordinates have been deposited in the Brookhaven Protein Data Bank (ID code 1afz).

* Author to whom correspondence should be addressed: telephone, (919) 966-3263; FAX, (919) 966-2852; E-mail, carter@med.unc.edu.

[§] University of North Carolina at Chapel Hill.

[||] Glaxo-Wellcome.

[⊗] Abstract published in *Advance ACS Abstracts,* April 1, 1997.

[1] Abbreviations: CDA, cytidine deaminase; ADA, adenosine deaminase; DAC, 3-deazacytidine; ZEB, zebularine or pyrimidin-2-one riboside; ZEB-$H_2O$, zebularine 3,4-hydrate; FZEB, 5-fluorozebularine; DHZ, 3,4-dihydrozebularine; U, uridine; HU, uridine 3,4-hydrate.

S0006-2960(96)03091-7 CCC: $14.00 

imply that the complex of CDA with uridine should be stable for long time periods and that observation of the product complex in a crystal structure should present no major problems. The X-ray crystal structure of the CDA−uridine complex is of more than routine interest because of previous publications describing the comparable adenosine deaminase−inosine (ADA−inosine) product complex (Wilson & Quiocho, 1994; Shih & Wolfenden, 1996).[2]

Crystallogenesis of the *E. coli* cytidine deaminase presents a favorable opportunity for the study of complexes of the enzyme with active-site-directed ligands. Lattice contacts between enzyme molecules are mediated extensively by a small, amino-terminal domain whose connection to the core of the enzyme is flexible. Thus, perfusion of ligand-free CDA crystals with a variety of ligands almost invariably leads to complex formation. In the present experiments, we have prepared crystals and solved this structure by two independent pathways. We first cocrystallized cytidine deaminase with product, uridine. Later, ligand-free crystals were soaked with substrate, cytidine, generating the uridine complex *in situ*.

Data from the two types of crystals were reduced, and the two structures were refined, independently as described for previously published complexes (Xiang et al., 1995, 1996). These replicate results provide an estimate for the sizes of errors in the structures, relative to the differences we observe between the two product complexes and the two transition-state analog complexes previously solved. Consequently, additional statistical characterization can be performed on the structural conclusions. Moreover, despite the fact that significant changes occur within the active site, the crystals remain highly isomorphous, perhaps because of the flexibility of the lattice contacts. Indeed, the crystals tolerate the exchange of ligands, despite the fact that there is no evident path to or from the active site. As a consequence of this isomorphism, difference Fourier methods have revealed a number of subtle structural details in the complexes that we have previously described (Xiang et al., 1995, 1996).

The two crystal structures of the CDA·U complex, reported here, confirm that the product binds as a 4-ketopyrimidine. Moreover, the results provide important new information about catalysis. First, they reveal a binding site for the leaving amino group. Second, comparisons between this structure and those of CDA·ZEB and CDA·FZEB support the view that the carboxylate group of Glu 104 furnishes a shuttle to transfer the proton from the zinc-bound hydroxyl group to the leaving amino group. Finally, the N1−C1′ glycosidic bond assumes an apparently strained bond angle, 19° away from the plane of the pyrimidine ring in the enzyme−product complex. This observation suggests a plausible alternative explanation for the previous, apparently incorrect interpretation of the X-ray data for the ADA−inosine complex (Wilson & Quiocho, 1994). It also suggests that the products of both reactions may be destabilized by a similar distortion, thereby "spring-loading" them for release.

Table 1: Crystallographic Data for the CDA·U Complex

| | CDA·U | CDA·C(U) |
|---|---|---|
| data | | |
| resolution limit (Å) | 2.3 | 2.3 |
| no. of observations | 65003 | 115150 |
| no. of unique reflections | 24137 | 27280 |
| completeness (%) | 80 | 92 |
| $R_{merge}$ (%) | 7.5 | 8.0 |
| $\langle I \rangle / \sigma(I)$ (2.45−2.3 Å) | 2.3 | 2.8 |
| refinement | | |
| protein atoms | 2220 | 2220 |
| ligand atoms | 16 | 16 |
| zinc atom | 1 | 1 |
| ordered waters (Å) | 51 | 51 |
| rms bond length deviation (Å) | 0.009 | 0.010 |
| rms bond angle deviation (deg) | 2.5 | 2.7 |
| *R*-factor | 0.19 | 0.19 |

## EXPERIMENTAL PROCEDURES

Crystals of CDA·U were grown by vapor diffusion in hanging drops initially containing 14−20% saturated ammonium sulfate (pH 6.2) and 11−16 mg/mL protein previously equilibrated with 20 mM uridine, against 1.0−1.6 mL reservoirs of 32−45% saturated ammonium sulfate at 4 °C. Alternately, crystals of ligand-free CDA were grown from similar preparations lacking uridine and subsequently soaked for several days with 5 mM cytidine. They were subsequently also prepared by soaking pregrown crystals of ligand-free CDA with saturating concentrations of substrate cytidine. All crystals were isomorphous with those of the transition-state complex CDA·ZEB (Xiang et al., 1995), having space group $P3_121$ and unit cell dimensions of $a = b = 120.3$ Å, $c = 78.4$ Å, and $b = 120°$. Data were collected at room temperature using an RAXIS II image plate and Rigaku RU-200 rotating anode. Data collection is summarized in Table 1.

The CDA·ZEB model with ZEB deleted from the coordinate list was used to initiate refinements of CDA·U. After the first cycle of X-PLOR refinement (Brunger et al., 1987; Brunger, 1988) the uridine was identified by a strong piece of electron density in the $\{|F_o| - |F_c|, \phi_{calc}\}$ difference Fourier map, with an orientation and shape very similar to that of ZEB in the CDA·ZEB complex. Furthermore, a well-resolved spherical electron density peak, close to C4 of uridine and between the backbone carbonyl of Thr 127 and the carboxylate of Glu 104, was found. It is located near the binding site for the incoming amino group of DAC observed in the CDA·DAC complex (Xiang et al., 1996). It was interpreted as a molecule of water or ammonia and refined as an oxygen atom. Between refinements, which were carried out first with X-PLOR and then with TNT (Tronrud et al., 1987), the model was rebuilt from both $2F_o - F_c$ and $F_o - F_c$ maps using FRODO (Jones, 1985). Water molecules were added after the *R*-factor at 2.3 Å resolution had reached a value less than 23%, and manual rebuilding did not improve the matches between the map and the model. Special care was taken with ligands in the active site, for

[2] X-ray data for the ADA−inosine complex were interpreted in terms of a model in which the ligand was a hydrated, tetrahedral *gem*-diolate structure and presented as a model for a transition state for the water exchange reaction (Wilson & Quiocho, 1994). On the basis of the slow rate of oxygen exchange, such a complex was recognized as unlikely to be stable, and $^{13}C$ NMR measurements showed no evidence in solution at neutral pH for the rehybrization of the scissile carbon atom for product complexes of either adenosine deaminase or cytidine deaminase (Shih & Wolfenden, 1996). The X-ray data presented by Wilson and Quiocho for the bound *gem*-diolate compound appeared persuasive, however, raising concern regarding the reliability of detailed structural analyses of enzyme−ligand complexes by means of X-ray crystallography and the possibility that lattice forces might have stabilized that rare species in the crystal.

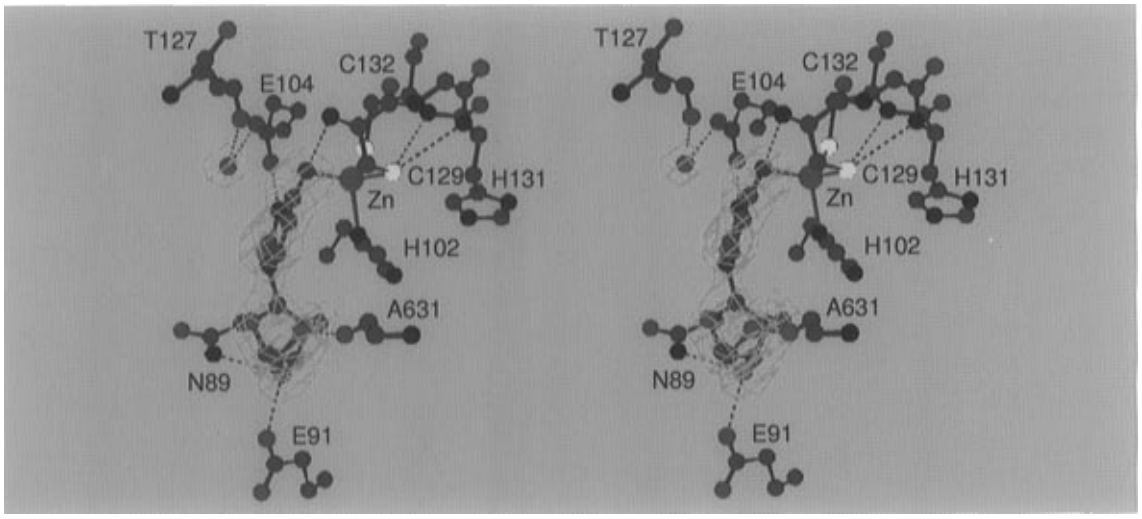


FIGURE 1: $\{|F_o| - |F_c|, \phi_c\}$ omit difference map at the active site showing well-resolved electron density peaks, contoured at 4$\sigma$, for the water molecule/leaving ammonium and for the product uridine.

which stereochemical parameters are less certain. Bond length constraints involving the zinc atom and its ligands were adjusted within reasonable ranges to satisfy the criteria that the $F_o - F_c$ map should be flat. The refinement statistics are listed in Table 1.

## RESULTS

The overall crystal structure of the complex CDA·U is, except at the active site, essentially identical to those of the ground-state complex CDA·DAC (Xiang et al., 1996), the pre-transition-state complex CDA·DHZ (Xiang et al., 1995), and the transition-state complexes CDA·ZEB and CDA·FZEB (Betts et al., 1994). Comparisons between the final refined coordinates indicate that rms deviations between CDA·U and those previously solved structures are 0.15−0.17 Å for backbone atoms and 0.44−0.46 Å for side chains. No significant variation was observed at specific residues, a conclusion which is also confirmed by the fact that no significant peaks or holes were found, except at the active site, in the $\{|F_{CDA\cdot U} - F_{CDA\cdot DAC}|, \phi_{CDA\cdot DAC}\}$, $\{|F_{CDA\cdot U} - F_{CDA\cdot DHZ}|, \phi_{CDA\cdot DHZ}\}$, $\{|F_{CDA\cdot U} - F_{CDA\cdot FZEB}|, \phi_{CDA\cdot FZEB}\}$, and $\{|F_{CDA\cdot U} - F_{CDA\cdot ZEB}|, \phi_{CDA\cdot ZEB}\}$ difference Fourier maps.

*A Binding Site for the Leaving Ammonia Molecule.* In the final refined structure, a peak of electron density that could represent the leaving ammonia or a water molecule (Figure 1) is located in a pocket previously identified as a binding site for the incoming amino group (Xiang et al., 1996). The electronegative atom presumed to be at this position forms two hydrogen bonds: one to the backbone carbonyl group of Thr 127 (3.0 Å) and another to the carboxylate group of Glu 104 (2.9 Å). In all complexed CDA structures we have examined (Betts et al., 1994, Xiang et al., 1995, 1996), the carbonyl oxygen of Thr 127 has an appropriate orientation for hydrogen bonding to the occupant of this binding site, which, for convenience in discussion, we will refer to as the leaving ammonia group. In earlier work, the carboxylate of Glu 104 was observed to form a hydrogen bond with the zinc-bound hydroxyl group in the ground-state, pre-transition-state, and transition-state complexes. Mutation of this residue to alanine reduces $k_{cat}/K_M$ by $10^8$-fold, and the activity can be rescued to a limited extent by formic acid (Carlow et al., 1996). In addition to its critical role in transition-state stabilization, Glu 104 appears to form a hydrogen bond with the leaving group in the product complex, playing the role of proton shuttle by transferring a proton from the zinc-bound hydroxyl group to the leaving group, as discussed later.

*Uridine Binds as the 4-Keto Pyrimidine.* Adenosine deaminase has been reported to bind the product inosine as inosine 1,6-hydrate (Wilson & Quiocho, 1994). This molecule is similar in structure to the expected transition state in oxygen exchange from water into the C═O group of inosine, a reaction previously shown to be catalyzed by adenosine deaminase (Wolfenden & Kirsch, 1968). The reported accumulation of this transition-state-like species on the enzyme was surprising because of the extremely unfavorable free energy of formation (Shih & Wolfenden, 1996).

CDA, like ADA, has recently been found to catalyze oxygen exchange from water into the product, uridine (D. Carlow, personal communication). In the present structure, the product uridine is not bound as the corresponding 3,4-hydrate. Rather, it is bound as the 4-ketopyrimidine, uridine, along with a molecule of water or ammonia. This is indicated by the well-resolved spherical electron density peak of the leaving group and the van der Waals contact distance (2.8 Å) between the center of this peak and the C4 of uridine. If the uridine 3,4-hydrate had been formed, a single bond (1.45 Å) between the leaving group and the C4 carbon atom should have been observed. However, in view of the possibility that the final X-ray structure is strongly biased toward the initial interpretation of the electron density (Read, 1997), especially at the current resolution (2.3 Å), it is reasonable to examine this point carefully.

To test the correctness of our structure, we repeated the refinement processes based on the alternative interpretation that a *gem*-diolate was bound. Starting from the CDA·ZEB structure model with ZEB deleted, one cycle of X-PLOR refinement was first carried out. Then, in separate experiments, the uridine (U) and uridine 3,4-hydrate (HU) were built into the electron density, and independent refinements were initiated for the two models. Both refinement processes were carried out using similar protocols as described under Experimental Procedures. Not surprisingly, cross-validation using the free *R*-value (Brunger, 1992) failed to distinguish between the refinements. Both $R_{free}$ and the crystallographic *R*-factor for the final models suggested a marginal preference

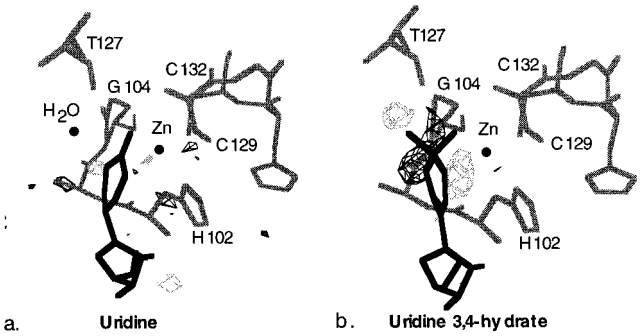


FIGURE 2: Residual $\{|F_o| - |F_c|, \phi_{calc}\}$ difference Fourier maps confirming that uridine (U) instead of its 3,4-hydrate (HU) is formed when it binds to CDA. (a) CDA·U, contoured at $2\sigma$; (b) CDA·HU, contoured at $3\sigma$.

for the incorrect structure, uridine 3,4-hydrate ($R_{free} = 0.225$, $R = 0.184$) over uridine ($R_{free} = 0.229$, $R = 0.186$). This result reinforces the notion that model bias can create the impression of having chosen the correct model.

The proper diagnostic in this case must be the residual maps calculated with coefficients $\{|F_o - F_c|, \phi_{calc}\}$ without omitting any atoms from the structure. In our structure refinements, $|F_o - F_c|$ difference maps are used extensively as a criterion to assess the reliability of the model and the convergence of the refinements. The residual difference Fourier map calculated from the final test CDA·U model shows no peaks near the active site when contoured at $3\sigma$ and small, uncorrelated noise peaks if the contour level is reduced to $2\sigma$ (Figure 2a). In contrast, the difference map calculated from the CDA·HU model (Figure 2b) indicates correlated positive and negative densities at $3\sigma$ sandwiching the O4b atom and the pyrimidine ring. The positive and negative densities around the O4b atom imply that the distance between the O4b and C4 atoms is longer than the single bond length of 1.45 Å in the model, indicating that no bond is formed between them. The positive and negative densities around the pyrimidine ring confirm the bending of the C1′−N1 glycosidic bond. This map provides the most convincing evidence regarding the correct structure. It contradicts the assumed gem diolate model and thus cannot arise from model bias. Thus, residual $|F_o - F_c|$ difference maps unambiguously indicate that uridine, rather than its 3,4-hydrate, is the correct model.

The omit map (Figure 1), the residual difference density, and the refined coordinates indicate that the pyrimidine ring and the C1′−N1 glycosidic bond are about 19° away from the expected coplanar configuration. Various implications of this unusual result are discussed below.

The identity of the peak at the expected location of the leaving ammonia molecule is of potential interest, since the crystals were grown in concentrated (0.8M) ammonium sulfate. $N^4$-methylcytidine is a good substrate for CDA (Cohen & Wolfenden, 1971b), suggesting that the methyl analog might be detectable at the active site by difference Fourier methods. We attempted unsuccessfully to identify this peak as an ammonia molecule or the corresponding cation by preparing the crystals in methylammonium sulfate. The absence of extra difference density implies that neither methylammonia nor the corresponding cation were bound. Since steric overlap of the extra methyl group might destabilize binding of that leaving group, this peak could still represent either ammonia, a bound water molecule, or an ammonium cation. The latter might be favored by electrostatic interaction with the carboxylate group of Glu 104.

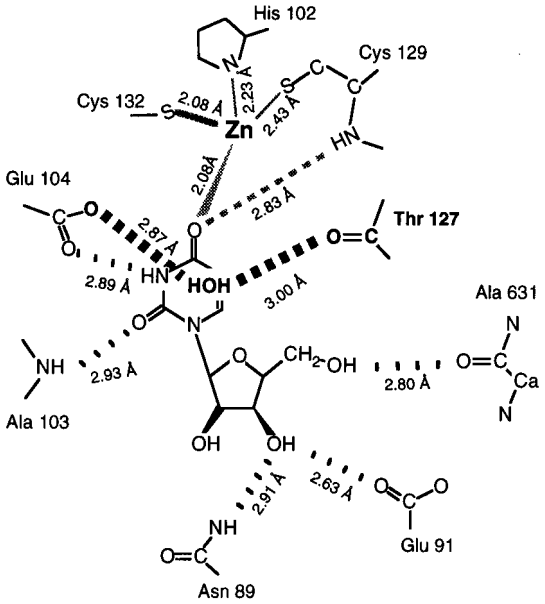


FIGURE 3: Schematic diagram of the CDA−uridine−ammonia/water complex. Hydrogen-bonding distances are indicated in angstroms along the bonds.

*Active Site Configuration.* The active site region in the product complex is shown schematically in Figure 3. The carboxylate group of Glu 104 makes quite different interactions with the product uridine compared with those observed in the ground-state (Xiang et al., 1996), the pre-transition-state (Xiang et al., 1995), and the transition-state (Betts et al., 1994; Xiang et al., 1995) complexes. The hydrogen bond between the carboxylate group of Glu 104 and O4/zinc-bound hydroxyl group observed in the other complexes is not found in CDA·U (Figure 4a). Instead, the carboxylate group of Glu 104 pivots about its $O_{\epsilon 1}$ oxygen atom in such a way as to leave the hydrogen bond between N3 and $O_{\epsilon 1}$ of Glu 104 essentially intact, while the $O_{\epsilon 2}$ atom moves toward the leaving group to form a hydrogen bond. The $O_{\epsilon 2}$ shifts 1.1 Å relative to the transition-state-like complex, CDA·ZEB. These relative shifts in the refined structures are confirmed by $\{|F_{CDA\cdot U} - F_{CDA\cdot ZEB}|, \phi_{CDA\cdot ZEB}\}$ (Figure 4b) difference Fourier maps with the inhibitor ZEB omitted from the structure factor phase calculation. The unambiguous rotation of the Glu 104 carboxylate group, away from the zinc-bound hydroxyl group toward the site occupied by the second leaving group, provides additional evidence that the O4 oxygen has assumed the keto configuration, in which it would no longer act as a hydrogen-binding partner to the carboxylate group.

The remaining interactions observed between the hydrated FZEB and ZEB inhibitors and the enzyme are also found in CDA·U (Figure 4a). These include the covalent bond between O4 and the zinc, the hydrogen bond between O4 and the backbone amide nitrogen of Cys 129, the hydrogen bond between $O_{\epsilon 1}$ of Glu 104 and N3 on the pyrimidine ring, and hydrogen bonds between the ribose 3′ and 5′ hydroxyl groups and residues 89, 91, and 631 across the dimer interface.

The Zn−$S_{\gamma 132}$ bond shortens as the reaction proceeds from transition state to product, as indicated by the positive density

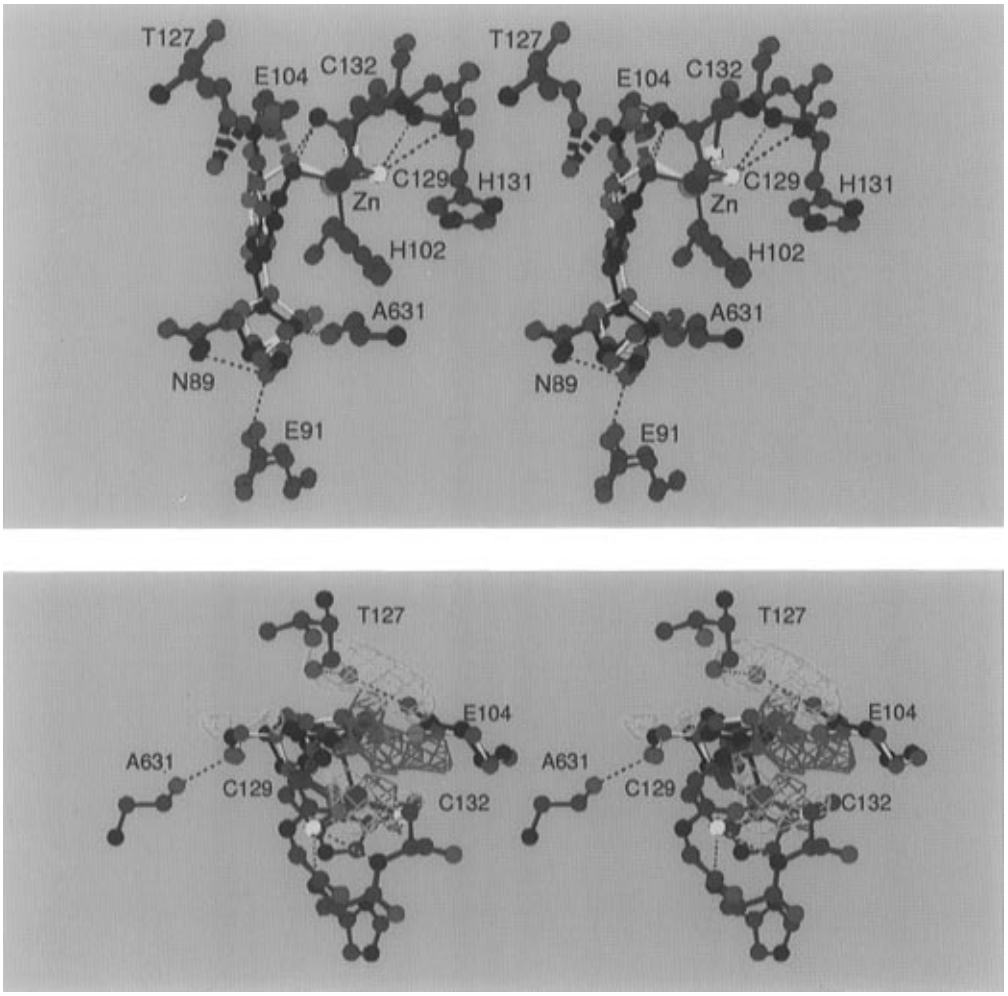


FIGURE 4: (a, top) Active site superposition of the transition-state complex CDA·ZEB and the product complex CDA·U. Significant structure changes are located at the carboxylate group of Glu 104. (b, bottom) Superposition of CDA·ZEB and CDA·U on the difference Fourier map calculated using coefficients $\{|F_{CDA\cdot U}| - |F_{CDA\cdot ZEB}|, \phi_{CDA\cdot ZEB}\}$, contoured at $4\sigma$, which indicates that the carboxylate of Glu 104 moves away from the zinc−water and toward the leaving amino group. Positive contours are in green and negative contours in red.

peak around that bond in the difference map $\{|F_{CDA\cdot U}| - |F_{CDA\cdot ZEB}|,\phi_{CDA\cdot ZEB}\}$ (Figure 4b). This bond was found to lengthen progressively during approach to the transition state, as inferred from the corresponding analog complexes, CDA·DAC, CDA·DHZ, and CDA·ZEB. It has been proposed that increasing the $Zn-S_{\gamma 132}$ bond length serves to buffer the net negative charge of the zinc coordination sphere, compensating for developing negative charge on the zinc-bound water, as the reaction proceeds toward the alkoxide-like state of highest negative charge in the transition state (Xiang et al., 1996). A similar inference can be drawn from the uridine complex. On the basis of the valence buffer model, conversion of transition state to product would be expected to reduce the negative charge on the 4-keto oxygen, so the observation that the $Zn-S_{\gamma 132}$ bond shortens in the product complex reinforces the proposal that this bond plays a valence buffering role during catalysis.

## DISCUSSION

*$NH_3$ Binding Site and the Proton Shuttle, Glu 104.* A striking feature of the CDA·U complex is that the leaving group peak occupies the same pocket as its progenitor analog, the 4-amino group of DAC in the ground-state complex CDA·DAC. Furthermore, both form hydrogen bonds to the backbone carbonyl oxygen of Thr 127. Comparison between the two structures indicates that the present peak is 0.5 Å further from the zinc atom than is the 4-amino group of DAC. Thus, it is likely that the leaving amino group moves slightly further away from the zinc during the reaction. The reaction seems to proceed by movement of the pyrimidine ring toward the zinc-bound water nucleophile, leaving the ammonia behind (Figure 5). The distinct movement of the ammonia molecule suggests that it is pulled simultaneously in the opposite direction.

The backbone carbonyl oxygen of Thr 127 has an appropriate orientation for hydrogen bonding to occupants of this leaving group site in all complex structures we have solved. Its orientation is fixed by the restricted $\phi$ rotation of Pro 128, a residue that is absolutely conserved in a broad spectrum of cytidine nucleoside and nucleotide deaminases (Betts et al., 1994). The role of this backbone carbonyl oxygen in binding both the N4 amino group and the leaving ammonia molecule may account for the conservation of this proline in cytidine deaminases (Betts et al., 1994; Carter, 1995).

As mentioned earlier, the hydrogen-bonding partner of the Glu 104 carboxylate $O_{\epsilon 2}$ oxygen atom switches from the zinc-bound hydroxyl group in the transition state complexes to the water molecule/ammonia in the product complex. Together with the observed reorientation of the Glu 104 carboxylate, formation of this hydrogen bond to the presumptive leaving group supports the previous suggestion

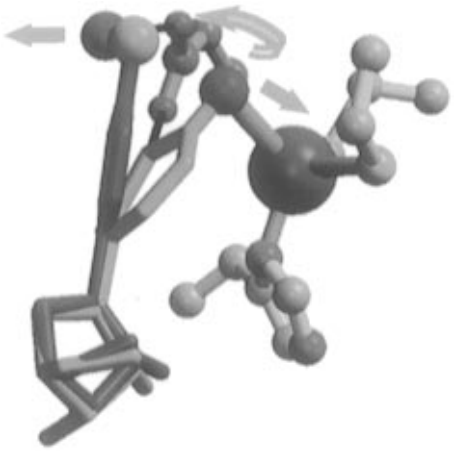

FIGURE 5: Overall trajectory of CDA-catalyzed deamination. The substrate analog deazacytidine (blue) is superimposed on the products uridine (green) and ammonia (blue). The pyrimidine moiety moves by 30° to the right toward the zinc, while the ammonia moves 0.8 Å to the left. The hydrogen-bonding configuration changes by rotation of the Glu 104 carboxylate group which leaves the O4 oxygen atom to form a hydrogen bond to the group in the leaving group pocket.

(Betts et al., 1994) that Glu 104 functions as a proton shuttle. In the product complex, the distance between the ammonia nitrogen atom and the zinc-bound carbonyl oxygen atom O4 is 2.9 Å, a van der Waals contact between nitrogen and oxygen. The Glu 104 carboxylate group is almost coplanar with the pyrimidine ring in the transition-state analog complex. Thus, it appears ideally positioned to extract a proton from the hydroxyl group to generate an enolate O4 alkoxide as an intermediate in the tautomerization to the 4-keto configuration. Furthermore, the short (2.48 Å) length of the hydrogen bond observed in transition-state analog complexes (Xiang et al., 1995) implies that the carboxylate group of Glu 104 may share the O4 proton almost equally with the zinc-bound hydroxyl group in that state. Reorientation of the Glu 104 $O_{\epsilon 2}$ atom presumably facilitates the breakdown of the transition state to both products, promoting both the enol-to-keto tautomerization of the pyrimidine and protonation of the leaving group in one deft maneuver.

Glu 104 is therefore a surprisingly versatile residue, which nearly single-handedly carries out each of the chemical transformations of the scissile 3−4 double bond in the substrate. In all structures we have solved (except for the complex with DAC which has a carbon atom in position 3 of the pyrimidine), the Glu 104 carboxylate was observed to form a hydrogen bond to the pyrimidine N3 atom, implying a role in protonation of that site early in the reaction, and then later to the zinc-bound hydroxyl group, stabilizing the transition state. The present findings indicate that the fate of the second proton from the substrate water is to be transferred to the leaving amino group by the same functional group. In the light of each of these roles, it is hardly surprising that mutation of Glu 104 to alanine cripples the enzyme, reducing its catalytic efficiency by a factor of $10^{-8}$ (Carlow et al., 1996).

*Distortion of the Glycosidic Bond Angle and Product Release.* The movement of the pyrimidine ring through a 30° trajectory from the configuration observed in the DAC complex (Figure 5) culminates in retention of the bond between the O4 keto oxygen atom and the zinc ion. The relative rigid body movements evident in the series of ligands we have studied (Betts et al., 1994; Xiang et al., 1995, 1996) are tabulated in Table 2. These movements indicate that the ribose moiety is rather firmly anchored within the active site. Progressive rotations of the pyrimidine by ∼20° in the transition-state complex and ∼30° in the product are considerably greater than those involving the ribose moiety, which average 5.6° ± 2.6°. The considerable torque imposed on the ribose moiety by differential movements of the ring is apparently resisted by hydrogen bonds between the O3′ oxygen atom and the side chains of Glu 91 and Asn 98 and the O5′ oxygen atom and the backbone carbonyl oxygen atom of residue 231 from the opposite subunit.

Table 2: Rigid-Body Analysis of Ligand Displacements

(A) Rotations[a] (in deg): Pyrimidine (Upper) and Ribose (Lower) Triangle

| CPD | DAC | DHZ | ZEB | FZEB | URID |
|---|---|---|---|---|---|
| DAC | | 11.4 | **22.9** | **23.3** | **28.7** |
| DHZ | 6.1 | | **22.9** | **22.4** | **29.9** |
| ZEB | **8.7** | 4.5 | | **1.97**[c] | **13.2** |
| FZEB | **10.6** | 4.0 | **3.6**[c] | | **13.2** |
| URID | 6.2 | 1.6 | 6.1 | 5.0 | |

(B) Translations[b] (in Å): Pyrimidine (Upper) and Ribose (Lower) Triangle

| CPD | DAC | DHZ | ZEB | FZEB | URID |
|---|---|---|---|---|---|
| DAC | | 0.503 | **1.049** | **1.023** | **0.735** |
| DHZ | 0.258 | | 0.667 | 0.576 | 0.634 |
| ZEB | 0.462 | 0.289 | | **0.242**[c] | 0.597 |
| FZEB | 0.297 | 0.168 | **0.299**[c] | | 0.595 |
| URID | 0.268 | 0.305 | 0.518 | 0.281 | |

[a] Rigid-body rotations were evaluated separately for ribose and pyrimidine ring atoms using the program CDSFIT (Daresbury Laboratory, 1990) for all possible pairs. [b] Root-mean-squared displacements were calculated similarly for all pairs of ribose and pyrimidine groups using EXCEL (Microsoft, 1993). [c] Values for ZEB and FZEB represent almost exactly the same state and are estimates of the noise in the calculation. These values and those which exceed them by 2.5$\sigma$ for translations and ribose rotation and by 10$\sigma$ for pyrimidine ring rotation are in boldfaced.

In the uridine complex we see evidence that the ribose binding pocket cannot accommodate the full reorientation of the pyrimidine ring that is required in order for the transition state to collapse to the keto form with the O4 oxygen atom bonded to the zinc. The 19° distortion of the C1′−N1 glycosidic linkage appears to be a compromise between breaking the O4−zinc bond, on the one hand, and breaking the ribose−active site hydrogen bonds, on the other hand. We can estimate the energy of this distortion from molecular mechanics, from structures in the small molecule database, and from quantum mechanical simulations. The molecular mechanics module in X-PLOR suggests that this distortion involves an energetic cost of ∼700 cal/mol. A survey of 6100 compounds in the Cambridge Small Molecule database reveals a small, but significant number of compounds in which a comparable distortion has been observed. Finally, semiempirical quantum mechanical calculations for the distortion of pyrimidine compounds (James Lewis, unpublished) show the expected coplanarity of the C1′−N1 bond with the ring but also show that it represents a broad energy minimum. Distortions of several tens of degrees can be expected to involve energies of less than 1 kcal/mol. From these estimates, it seems reasonable that the angle between the glycosidic bond and the pyrimidine ring can be distorted with very modest costs in energy.

The O4−zinc bond might in principle be expected to pose a barrier to product dissociation (as it certainly does to dissociation of the transition-state analog, zebularine hydrate). An intriguing possibility raised by the strained glycosidic bond angle is that securing the ribose hydroxyl groups to hinder the formation of a planar 4-ketopyrimidine could weaken the O4−zinc bond, destabilizing the uridine complex relative to that for undistorted uridine, promoting product release.

Wilson and Quiocho (1994) described an unusual *gem*-diolate adduct as their interpretation of X-ray data from a comparable adenosine deaminase−inosine complex. This interpretation was shown to be unlikely for both ADA and CDA by $^{13}C$ NMR measurements in which the reaction products retained their $sp^2$ hybridization (Shih & Wolfenden, 1996). In the present context, we note that if the pyrimidine ring were restored to coplanarity with the C1′−N1 glycosidic bond, the C4 atom would reside nearly exactly midway between the positions of the oxygen atoms on either side of the ring. We propose that an underlying reason for this apparently mistaken interpretation may have been that the C1′−N9 glycosidic linkage of inosine might also actually be bent in the ADA−inosine complex. The attempt to impose planarity and refining that structure could have positioned the purine ring midway between the zinc-bound oxygen and an occupant of a corresponding leaving group site in ADA. Our refinement of such an incorrect configuration for the CDA−uridine complex shows that model phase bias leads to an apparent convergence of this erroneous refinement with statistics indistinguishable from those of the correct structure. The final arbiter of the correct structure always should be the residual $\{|F_o| - |F_c|, \phi_{calc}\}$ difference Fourier synthesis.

The present crystal structure of the CDA−uridine complex completes a series of CDA−ligand complexes tracing the structural changes encountered during catalysis. This structural reaction profile has revealed substantial new subtleties about the reaction mechanism. The active site provides attractive forces that pull the two products away from one another (Figure 5). The pyrimidine ring moves toward the zinc-activated water molecule while the 4-amino group moves in the opposite direction into a leaving group pocket formed by the conformationally restricted carbonyl oxygen atom of Thr 127. This molecular leverage is exerted around a fulcrum in which a hydrogen-bonded network anchors two of the ribose hydroxyl groups. A consistent pattern of changes in the length of the $S_{\gamma 132}$−zinc bond provides a mechanism for adjusting the electrophilicity of the zinc ion to the increase and loss of negative charge on the activated water molecule, buffering its interactions with other zinc ligands and with the carboxylate group of Glu 104.

The affinities of cytidine and uridine for solvent water (Cullis & Wolfenden, 1981) reveal that uridine is, surprisingly, roughly 2 orders of magnitude less well solvated than is cytidine. This difference suggests that, in the absence of a mechanism for expelling the product, uridine might reduce catalytic throughput by remaining tightly bound to CDA. The present structure appears to uncover the structural basis for a more substantial product destabilization than is evident in the substrate analog complexes of CDA (Xiang et al., 1995, 1996). Once formed, the product uridine finds itself cramped between simultaneous constraints, the O4−zinc bond at one end and the anchored ribose at the other, which may destabilize the ground-state product complex and promote its release.

## REFERENCES


Ashley, G. W., & Bartlett, P. A. (1984) *J. Biol. Chem. 259*, 13621−13627.

Betts, L., Xiang, S., Short, S. A., Wolfenden, R., & Carter, C. W. J. (1994) *J. Mol. Biol. 235*, 635−656.

Brunger, A. (1992) *Nature 355*, 472−474.

Brunger, A. T. (1988) *The X-PLOR Manual*, The Howard Hughes Medical Institute and Department of Molecular Biophysics and Biochemistry, Yale University, New Haven, CT.

Brunger, A. T., Kuriyan, J., & Karplus, M. (1987) *Science 235*, 458.

Carlow, D., Short, S. A., & Wolfenden, R. (1995) *Biochemistry 34*, 4220−4224.

Carlow, D. C., Short, S. A., & Wolfenden, R. (1996) *Biochemistry 35*, 948−954.

Carter, C. W., Jr. (1995) *Biochimie 77*, 92−98.

Cohen, R. M., & Wolfenden, R. (1971a) *J. Biol. Chem. 246*, 7561−7565.

Cohen, R. M., & Wolfenden, R. (1971b) *J. Biol. Chem. 246*, 7566−7568.

Cullis, P. M., & Wolfenden, R. (1981) *Biochemistry 20*, 3024−3028.

Daresbury Laboratory (1990) *The CCP4 Program Suite*, Daresbury Laboratory, Warrington WA4 4AD, U.K.

Frick, L., MacNeela, J. P., & Wolfenden, R. (1900) *Bioorg. Chem. 15*, 100−108.

Jones, T. A. (1985) *Methods Enzymol. 115*, 157−171.

Kim, C. H., Marquez, V. E., Mao, D. T., Haines, D. R., & McCormack, J. J. (1986) *J. Med. Chem. 29*, 1374−1380.

Liu, P. S., Marquez, V. E., Driscoll, J. S., Fuller, R. W., & McCormack, J. J. (1981) *J. Med. Chem. 24*, 662−666.

Marquez, V. E., Liu, P. S., Kelley, J. A., Driscoll, J. S., & McCormack, J. J. (1980) *J. Med. Chem. 23*, 713−715.

Microsoft (1993) Microsoft Corp., Seattle, WA.

Read, R. J. (1997) *Methods Enzymol.* (in press).

Shih, P., & Wolfenden, R. (1996) *Biochemistry 35*, 4697−4703.

Tronrud, D., Ten Eyck, L. F., & Mathews, B. W. (1987) *Acta Crystallogr. A43*, 489−501.

Wilson, D. K., & Quiocho, F. A. (1993) *Biochemistry 32*, 1689−1694.

Wilson, D. K., & Quiocho, F. A. (1994) *Nat. Struct. Biol. 1*, 691−694.

Wilson, D. K., Rudolph, F. B., & Quiocho, F. A. (1991) *Science 252*, 1278−1284.

Wolfenden, R., & Kirsch, J. F. (1968) *J. Am. Chem. Soc. 90*, 849−850.


BI963091E